Journal of Energy Chemistry 26 (2017) 942–947

Contents lists available at ScienceDirect

Journal of Energy Chemistry

journal homepage: www.elsevier.com/locate/jechem

http://www.journals.elsevier.com/journal-of-energy-chemistry/

NiO–CaO materials as promising catalysts for hydrogen production through carbon dioxide capture and subsequent dry methane reforming

Alejandra Cruz-Hernández, J. Arturo Mendoza-Nieto, Heriberto Pfeiffer*

Laboratorio de Fisicoquímica y Reactividad de Superficies (LaFReS), Instituto de Investigaciones en Materiales, Universidad Nacional Autónoma de México, Circuito exterior s/n, Ciudad Universitaria, Del. Coyoacán, CP 04510, Ciudad de México, Mexico

ARTICLE INFO

Article history:
Received 23 May 2017
Revised 29 June 2017
Accepted 2 July 2017
Available online 6 July 2017

Keywords:
Methane reforming
CO_2 capture
Calcium oxide
H_2 production
NiO supported

ABSTRACT

In this work, CaO-NiO mixed oxide powders were evaluated as consecutive CO_2 chemisorbents and catalytic materials for hydrogen production thought the CH_4 reforming process. Between the NiO-impregnated CaO and CaO–NiO mechanical composite, the first one presented better chemical behaviors during the CO_2 capture and CH_4 reforming processes, obtaining syngas ($H_2 + CO$) as final product. Results showed that syngas was produced at two different temperature ranges, between 400 and 600 °C and at $T > 800$ °C, where the first temperature range corresponds to the CH_4 reforming process but the second temperature range was attributed to a different catalytic reaction process: CH_4 partial oxidation. These results were confirmed through different isothermal and cyclic experiments as well as by XRD analysis of the final catalytic products, where the nickel reduction was evidenced. Moreover, when a $CO–O_2$ flow was used during the carbonation process a triple process was achieved: (i) CO oxidation, (ii) CO_2 chemisorption and (iii) CH_4 reforming. Using this gas flow the hydrogen production was always higher than that obtained with CO_2.

1. Introduction

Nowadays, the anthropogenic emissions of carbon dioxide (CO_2) and other green-house gases (GHG) have triggered the global climate change [1–3]. Based on that, the demands for energy alternatives have grown, where the new energy sources must be environmentally friendly. Hence, developing clean alternative fuels, such as hydrogen is not the exception. Hydrogen is produced mainly from fossil fuels, biomass and water [4–21]. Specifically, in the fossil fuels and biomass processes the hydrogen production is performed through reforming of natural gas [5], thermal cracking of natural gas [6], partial oxidation of heavier hydrocarbons [7], or coal gasification [8]. On the contrary, if biomass is used for hydrogen production the most common methods are pyrolysis [9] or gasification [10], steam methane reforming (SMR), water–gas shift reaction (WGSR), dry methane reforming and ethanol-steam reforming [11–16].

An alternative clean fuel produced from carbon dioxide and methane during reforming reaction was patented by Williams in 1933 [17]. Later in 1963, Gorin and Retallik [18] patented the fluidized bed concept, using a two different materials: (1) a carbon dioxide acceptor and (2) a reforming catalyst, in order to produce hydrogen. In this line, recently it has been shown that different CO_2 sorbents [19], i.e., Na_2ZrO_3 can be used as bifunctional materials, acting first as a CO_2 captor and then as a catalytic material for methane reforming reaction, presenting a clearly advantages over the procedure proposed by Gorin and Retallik. Other CO_2 material captors, namely alkali (Li, Na and K) [20–25] and alkaline-earth (Be, Mg and Ca) [26–29] metal-based ceramics have shown high ability for CO_2 capture. Therefore, all these ceramics may be promissory carbonated materials for hydrogen production through dry methane reforming. Dry methane reforming reaction is represented in Eq. (1), where two greenhouse gases, CO_2 and CH_4, are used as reactants in order to produce the syngas mixture composed by CO and H_2.

$$CH_{4\,(g)} + CO_{2(g)} \rightarrow 2H_{2\,(g)} + 2CO_{\,(g)} \quad (1)$$

Up to now, calcium oxide (CaO) and nickel oxide supported over magnesium oxide (NiO/MgO) have been used already as materials for CO_2 capture [30–33] and for CO_2 reforming of CH_4 [34], respectively. Besides, the carbon dioxide removal in a single-reactor packed with a calcium oxide mixture was examined by Chun and Harrison [35]. An important application of CaO-based

* Corresponding author.
E-mail addresses: pfeifferperea@gmail.com, pfeiffer@iim.unam.mx (H. Pfeiffer).

http://dx.doi.org/10.1016/j.jechem.2017.07.002

sorbents is proposed for a vehicle use, where Specht et al. [36] reported its continuous hydrogen production system using two regenerative reformers via methane steam reforming. Kato et al. [37,38] have also reported that CaO-based sorbents. In this case, CaO was mixed with Ni particles and examined for CO_2 capture and methane steam reforming for a zero-emission fuel cell vehicle system. Also, mesoporous materials composed by NiO–CaO–Al_2O_3 have been synthetized, characterized and tested for CO_2 reforming of CH_4, showing large specific surface areas (between 100 and 230 m^2/g), good thermal stabilities at 700 °C and high catalytic activities [39]. On the other hand, CaO–NiO materials have been synthesized by some methods, such as mixing thoroughly [40], sol–gel [41], calcined precursors [42] and incipient impregnation [29]. However, there is little information about these composite abilities for sorption-reforming during dry CO_2 methane reforming reaction.

According to Jhonsen et al. [43], the sorption-enhances steam reforming (SEMR) can be performed using a calcium based CO_2 sorbent as it was demonstrated in previous work by Brun-Tsekhovoi et al. [44] in 1988. However, Balasubramanian et al. [45] provided significant more information by adding calcium oxide to commercial steam methane reforming (SMR) catalysts, which enhanced the H_2 production up to >95%, in a single-step process. In that single-step process the three simultaneous reactions occur in a fluidized bed reactor containing a mixture of reforming catalysts and CO_2 acceptor where the acceptor is cycled continuously.

Summarizing, there are few informations about NiO–CaO catalytic activity for hydrogen production through dry methane reforming. Therefore, the aim of this work was to determinate if materials composed by CaO and NiO can act sequentially as CO_2 captors and after as catalytic materials for hydrogen production. Additionally, it was analyzed if the carbonation conditions, using CO_2 or CO–O_2 fluxes, modify the catalytic performance of these materials during H_2 production.

2. Experimental

Calcium oxide (CaO) was obtained via calcination of calcium carbonate, while NiO-containing CaO samples were prepared by impregnation and mechanical mixing, respectively. The complete synthesis processes were described in a previous work [29]. Hereafter, these samples will be labeled as NiO-impregnated CaO and CaO–NiO mechanical composite. Samples were structurally and microstructurally characterized by powder X-ray diffraction (XRD) and N_2 physisorption [29]. The XRD patterns for NiO-impregnated CaO and CaO–NiO mechanical mixture samples exhibited reflections fitting the 37-1497 (CaO) and 47-1049 JCPDS-ICDD (NiO) cards, as it could be expected. Once the crystalline structure in both samples were determined, nitrogen adsorption–desorption isotherms were obtained. According to IUPAC classification, the materials presented type II isotherm related to nonporous materials with no hysteresis loop, with specific surface areas (S_{BET}) of 8 and 12 m^2/g for the NiO-impregnated CaO and CaO–NiO mechanical mixture, respectively. Finally, elemental characterization results showed that both samples have very similar CaO:NiO molar contents: 0.98:0.03 for NiO-impregnated CaO and 0.97:0.03 for the CaO:NiO mechanical composite samples.

Catalytic activity of both nickel-containing materials was tested for hydrogen production through two consecutive processes, as it was already described [19]. Carbon dioxide (CO_2) capture followed by dry methane (CH_4) reforming reactions was performed in a Bel-Rea catalytic reactor from Bel Japan, using 100 mg of sample. Regarding to the CO_2 capture, both materials were carbonated dynamically from 30 to 600°C, then isothermally treated at 600 °C for 1 h and finally cooled down until 200 °C, using two different gas mixtures: (i) 10 vol% CO_2 (Praxair grade 3.0) and 90 vol% N_2 (Praxair grade 4.8) and (ii) 5 vol% O_2 (Praxair, grade 2.6) and 5 vol% CO balanced with N_2 (Praxair, certified mixture). In both cases, total flow rates of 100 mL/min were employed. After the carbonation processes, dry methane reforming tests were performed with the previously carbonated samples from 200 to 900 °C with a heating rate of 2 °C/min using 100 mL/min of a gas mixture composed by 2 vol% of CH_4 (Praxair grade 5.0) balanced with N_2.

Cyclic experiments for CO_2 capture and subsequent dry reforming tests were performed with the NiO-impregnated CaO catalyst. Although the carbonation process was performed as in the previous experiments, two different experiment designs were tested during the reforming stage: (i) dynamic tests heating from 200 to 900 °C and (ii) isothermal tests at 600 °C for 70 min. These double procedure was performed during 5 cycles, adding a sixth cycle, where the CO_2 capture and CH_4 reforming processes were performed after a previous oxidation step under 30 mL of O_2 at 600 °C for 2 h. All the catalytic gas products were analyzed each 15 °C until 900 °C in dynamic experiments or each 8.3 min in isothermal experiments, using a Shimadzu GC 2014 gas chromatograph with a Carbonex-100 column. Moreover, all catalytic materials obtained after dry reforming experiments were characterized by powder X-ray diffraction.

3. Results and discussion

3.1. CH_4 reforming using CO_2 as CaO carbonation specie

A sequential process composed by a carbon dioxide capture at 600 °C followed by the catalytic conversion of CH_4 and the CO_2 previously captured to syngas ($H_2 + CO$) was performed and followed with gas chromatography, where two different samples were employed: NiO-impregnated CaO and NiO–CaO mechanical composite. It has to be mentioned that carbonation process was performed at 600 °C according to a previous report [29], where it was probed that NiO-impregnated CaO and NiO–CaO mechanical composite samples presented the highest CO_2 chemisorption efficiencies. Fig. 1 shows the concentration evolution of reagents CH_4 and CO_2 (desorbed from previous CaO carbonation) as well as the syngas products (H_2 and CO), presented in reactive efficiency (%). When the NiO-impregnated CaO sample was used as catalytic material, small quantities of CO_2 were evidenced between 500 and 650 °C, indicating that CO_2 is being desorbed from the CaO carbonated ceramic, but it is not totally converted to syngas (Fig. 1(a)). The CO_2 desorption is in good agreement with the CH_4 reforming process, as CH_4 gas concentration decreased in the same temperature range, while H_2 and CO increased. In fact, the highest hydrogen percentage (42.3%) was obtained at 630 °C, which corresponds to the formation of 1.7 sccm of hydrogen. At higher temperatures ($T > 800$ °C) a second set of hydrogen and carbon monoxide production can be observed, with the corresponding CH_4 reduction. However, in this temperature range, CO_2 was not detected.

The syngas production at the highest temperatures may be produced through a different reaction process, as CO_2 seems not to be present. In this case, the syngas may have been produced by the methane partial oxidation process. In fact, the XRD pattern (Fig. 2) obtained from the NiO-impregnated CaO sample after the catalytic process showed the presence of CaO (JCPDS-ICDD card 37-1497) as the main phase, but carbon (JCPDS-ICDD card 075-1621) and Ni metallic (JCPDS-ICDD card 004-0850) were detected as well. In fact, if these XRD patterns are compared with pristine samples [29], the only essential difference is the NiO phase evolution to metallic Ni. Thus, nickel reduction must have induced the methane partial oxidation (Eq. (2)). Moreover, in Fig. 1, it is evident that H_2 production is the double than CO, which is in good agreement with the CO evolution detected in this temperature range.

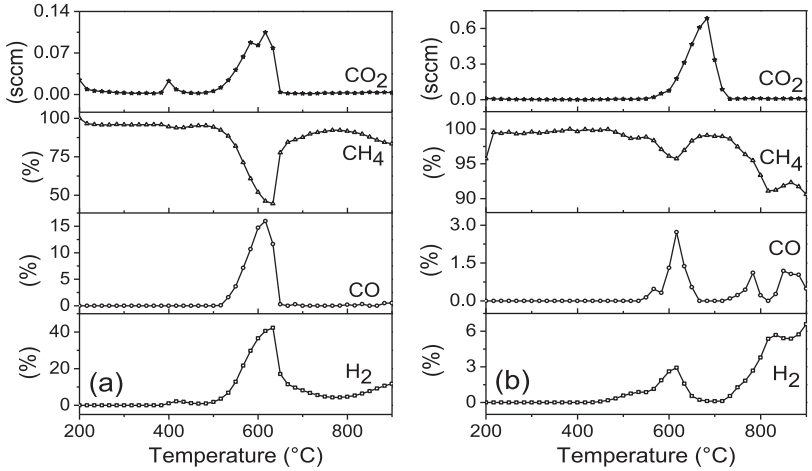

Fig. 1. Dynamic evolution of reactants (CO_2 and CH_4) and products (CO and H_2) obtained for CH_4 reforming process using (a) NiO-impregnated CaO material and (b) NiO–CaO composite. CO_2 average quantification is not possible, as it is desorbed from ceramic materials. Thus, CO_2 is only reported in sccm units.

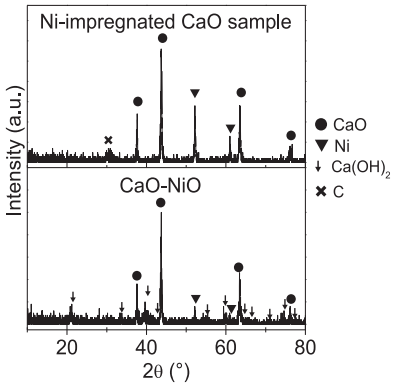

Fig. 2. X-ray patterns for CaO material impregnated with NiO and NiO–CaO composite after the CO_2 desorption and catalytic processes.

$$CH_{4(g)} + NiO_{(s)} \rightarrow 2H_{2(g)} + CO_{(g)} + Ni_{(s)} \quad (2)$$

A different catalytic behavior was observed for the CaO–NiO composite. The CH_4 content almost remain constant in all the dynamic process (Fig. 1(b)), indicating that the methane conversion with this sample was carried out in a minor degree, in comparison with the NiO-impregnated CaO sample. In this case, the CO_2 desorption from the composite took place between 600 and 730 °C, and it was, at least, six times higher than those obtained with the NiO-impregnated CaO sample. This result indicates that in the composite the desorption process occurs faster than in the CaO impregnated with Ni or the catalytic process is not taking place. In addition, Fig. 1(b) shows that H_2 formation was detected in two different temperature ranges: 500–650 °C and 730–900 °C. In the first temperature range, the H_2 production reaches 2.9% (0.12 sccm), that is almost 14 times lower than the H_2 production registered in the same temperature range for the NiO-impregnated CaO material (Fig. 1(a)). In this case, the highest amount of hydrogen (2.7 sccm) was obtained at 900 °C. It seems that hydrogen production is mainly generated at high temperatures through the methane partial oxidation process. As in the previous sample, the corresponding XRD pattern confirmed the nickel reduction process (Fig. 2). In this case, it was detected the presence of small amounts of $Ca(OH)_2$, which must be associated to a hydroxylation process produced during the sample handling. The above results clearly showed the catalytic advantages that NiO-impregnated CaO sample provides over the mechanical composite.

Fig. 3 shows scanning electron images displaying the NiO-impregnated CaO sample morphology before and after the catalytic process. As it was previously described [29], the morphology of this sample evidenced the NiO deposition and incrustation with particles sizes between 50 and 100 nm. These tiny particles were deposited over large CaO particles (~10 μm). After the CO_2 desorption and catalytic process, different morphological changes were evidenced. CaO particle samples seemed to present a higher corrugation, while the Ni-containing particles continued highly dispersed over the CaO surface. In this case, the Ni-containing particles did not seem to modify their particle size. Moreover, the carbon presence was evidenced by the formation of filament-like particles, which may have growth using the nickel nanoparticles as seeds. Therefore, it can explain why carbon was not produced, or at least evidenced, on the CaO–NiO composite.

In order to analyze the possible cyclability of the NiO-impregnated CaO material in the carbonation and subsequent CH_4 dynamic conversion to syngas, six cycles were performed into the physicochemical conditions previously described in the experimental section. Fig. 4 shows the hydrogen formation as function of temperature in each cycle. As in the previous experiment, two temperature ranges for H_2 production were observed between 500–700 °C and 800–900 °C, associated to the CH_4 reforming and CH_4 partial oxidation processes, respectively. CH_4 reforming (500–700 °C) depends strongly on the number of cycles performed. The main hydrogen production occurs at around 600 °C for all the cycles, where the highest hydrogen amounts decreases drastically from 40% to 19% in the first and second cycles, respectively. It corresponds to 47.5% of decrement in the hydrogen production. Then, cycles 3–5 showed a further decrease in the H_2 formation, until 11.1%, which was registered in the fifth cycle. The reason for the hydrogen production decrement may be due to different factors, such as NiO reduction to metallic nickel or carbon deposition over the particle surface (see XRD results, Fig. 2), inhibiting the catalytic process. All these factors and the physicochemical atmosphere conditions should have modified the CaO carbonation, reducing the CH_4 reforming process. In order to corroborate that the metallic Ni or carbon deposition were responsible of the phenomena observed in Fig. 4, a sixth cycle was performed with a previous oxidation stage (see experimental section), where hydrogen production increases from 11.1% to 24.8%, between the fifth and sixth cycles. In contrast, the catalytic performance in the highest temperature range (CH_4 partial oxidation) only decreased in 3%–5% during the cyclic tests, and the efficiency was recovered after the oxidation process. Therefore, the carbonation modifications, observed during

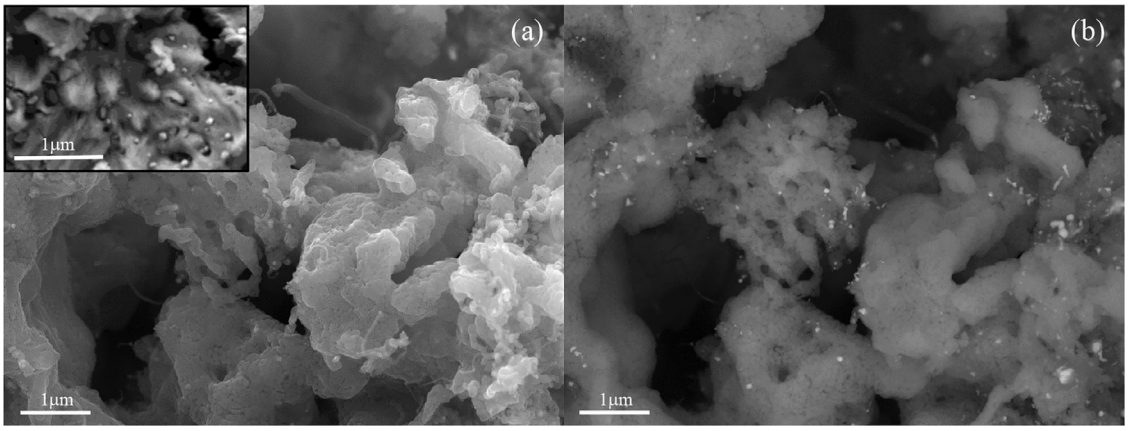

Fig. 3. Secondary (a) and backscattered (b) electron images for NiO-impregnated CaO sample obtained after the CO_2 desorption and catalytic processes. The square inset shows the original morphology of the sample.

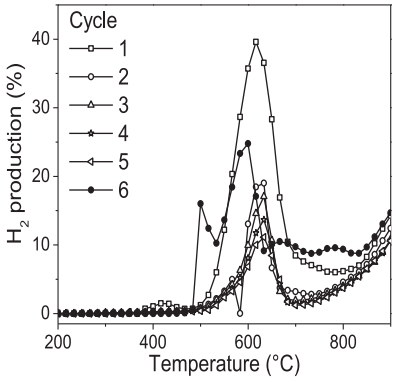

Fig. 4. Hydrogen dynamic evolution for six cycles of CO_2 carbonation-dry reforming, using the NiO-impregnated CaO sample.

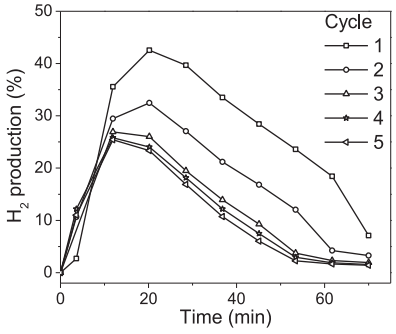

Fig. 5. Hydrogen evolution at 600 °C for five cycles of carbonation-dry reforming, using the NiO-impregnated CaO sample.

the CH_4 reforming process, did not modify the CH_4 partial oxidation as it does not depend on the CO_2.

Considering that in the dynamic process the highest amount of H_2 was obtained at 600 °C, different isothermal experiments were undertaken at this temperature. Fig. 5 shows the hydrogen formation as function of time for the fifth consecutive cycles performed. A similar catalytic behavior, than that observed in the dynamic tests, was registered for these isotherms. In the first cycle, the highest amount of H_2 was obtained (42.6%) after 20 min of reaction and then the percentage of H_2 formed decrease as function of time. The H_2 production decrement was generated due to the CO_2 content limitation in the sample. As the CH_4 reforming process depends on the CO_2 viability, the reaction can only be produced

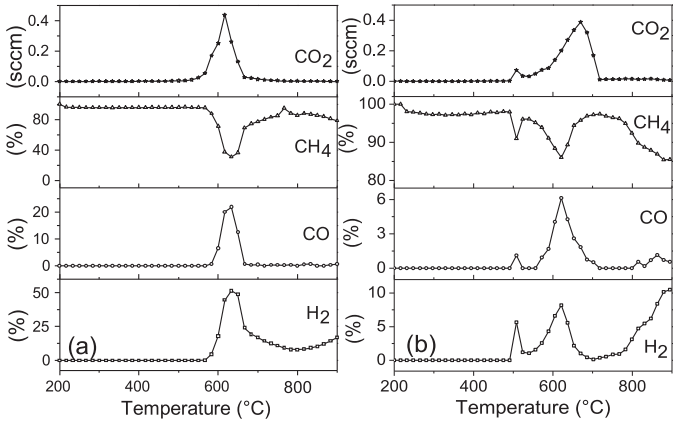

Fig. 6. Dynamic evolution of reactants (CO_2 and CH_4) and products (CO and H_2) obtained for CH_4 reforming process using (a) NiO-impregnated CaO material and (b) NiO–CaO composite. CO_2 average quantification is not possible, as it is desorbed from ceramic materials. Thus, CO_2 is only reported in sccm units.

during the time in which CO_2 is been desorbed. After the first cycle, a drastically H_2 formation decrease was observed during the following four cycles, and 23.3 % of H_2 production was obtained in the fifth cycle.

3.2. CH_4 reforming using CO and O_2 as CaO carbonation species

It was previously reported that CaO material is able to perform the CO oxidation and then capture the CO_2 produced in a wild range of temperatures (350–750 °C) [29]. Thus, in the present section a sequential process composed by a CO oxidation-CO_2 capture at 600 °C followed by the catalytic conversion of CO_2 and CH_4 to syngas mixture ($H_2 + CO$) was performed. Both samples composed by CaO and NiO were employed as catalytic materials for performing three consecutive processes: (i) CO oxidation, (ii) CO_2 capture and (iii) dry reforming reaction.

Fig. 6 shows the thermal reactive efficiency (%) evolution from 200 to 900 °C for reactants and products during the reforming reaction performed after the subsequent CO oxidation-CO_2 capture processes at 600 °C. For both samples, similar amounts of CO_2 (0.4 sccm) were desorbed. However, this process took place at different temperatures. In the CaO–NiO composite the CO_2 desorption occurred at 670 °C, whereas in the NiO-impregnated CaO sample, the maximum CO_2 desorption was reached at a lower temperature, 615 °C. On the contrary, the methane content presented two well defined decrements in both samples. The first CH_4

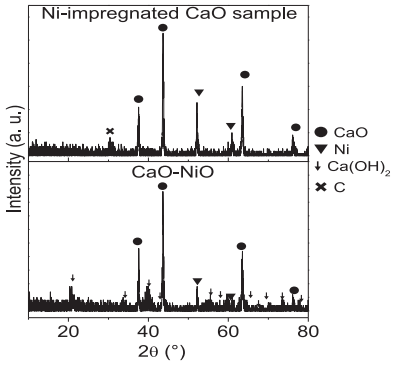

Fig. 7. X-ray patterns for CaO material impregnated with NiO and NiO–CaO composite after the CO_2 desorption (previously captured by the CO oxidation-chemisorption) and catalytic processes.

decrement occurred at around 510–530 °C and the second between 620 and 635 °C. Despite similar amounts of CO_2 were desorbed in both samples, the CH_4 reforming process was produced in higher proportion with NiO-impregnated material. Regarding to CO formation, the sample impregnated with Ni reached the highest amount (22%) at 630 °C, whereas with the CaO–NiO composite only produced 6.2% at 620 °C. Finally, from Fig. 6 it is possible to see that H_2 is produced with both samples. When NiO-impregnated CaO sample was used, the H_2 was detected since 580 °C. At higher temperatures than 580 °C, hydrogen formation became more evident; reaching its highest amount at 630 °C (51.3%). In contrast, the thermal evolution for CaO–NiO composite showed a lower CH_4 conversion and the H_2 production was obtained in the same temperature range (Fig. 6(b)). The H_2 production presents three maxima at 510, 620 and 900 °C. These three temperatures are in good agreement with the CH_4 reforming (first two temperature ranges) and the previously described CH_4 partial oxidation reaction (highest temperature). The above results clearly show that using a NiO-impregnated CaO sample benefits the H_2 formation at least five times in comparison with the CaO–NiO composite. Furthermore, these results are similar to those observed with the direct CO_2 carbonation (Fig. 1), where NiO-impregnated CaO sample presented the best catalytic behavior during CH_4 reforming, regardless the physicochemical conditions used during the previous carbonation step: (1) CO_2 chemisorption or (2) CO oxidation followed by a subsequent CO_2 chemisorption on calcium oxide.

Also, results from Figs. 1 and 6 can be compared in order to determinate which physicochemical conditions during the carbonation stage are the optimal for producing the highest amount of H_2 during dry methane reforming. Regardless the CaO sample used, when the CO oxidation-CO_2 capture processes took place during the carbonation stage, a significant increase in the H_2 formation was observed (Fig. 6) in comparison with the results obtained when the samples were directly carbonated with CO_2 (Fig. 1). For CaO–NiO composite an increase from 2.9% (Fig. 1) to 8.2% (Fig. 6) was observed at 620 °C, whereas an increase from 42.3% to 51.3% in H_2 production was obtained when the NiO-impregnated CaO sample was carbonated through CO oxidation and CO_2 storage. In both cases, values reported only correspond to the CH_4 reforming reaction.

In order to determine the sample composition after the triple process, both CaO materials were analyzed by XRD, where CaO and Ni metallic phases were detected in the corresponding NiO-impregnated CaO XRD pattern, as expected in Fig. 7. This result indicates that CaO can be regenerated. However, NiO was reduced into metallic nickel, which must modify the catalytic activity for the CH_4 reforming reaction.

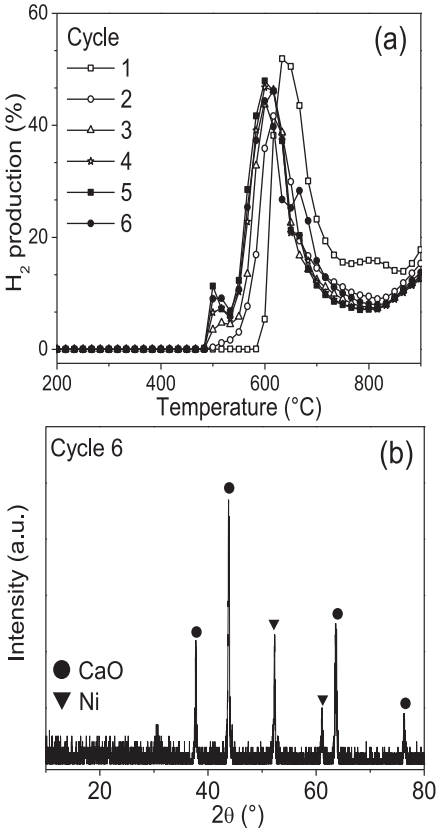

Fig. 8. Hydrogen dynamic evolution for six cycles of CO oxidation-CO_2 capture-dry reforming using the NiO-impregnated CaO sample (a) and X-ray pattern for the product obtained after six cycles (b).

After the initial results, several cycles for syngas production were performed, only using the NiO-impregnated CaO material. Fig. 8(a) shows the hydrogen formation as a function of temperature in consecutive cycles. Three temperature ranges for H_2 production were observed between 500–550, 550–750 and 800–900 °C. In the second temperature range (between 550 and 750 °C), the largest amounts for H_2 were obtained, reaching 51.9% of hydrogen in the first cycle at 630 °C. After the first cycle, the hydrogen production tended to decrease as a function of the cycles. Hydrogen production may have been reduced due to change in particle surfaces. However, it must be pointed out that this H_2 decrement observed among cycles (Fig. 8(a)) is lower than that observed in Fig. 4 when the NiO-impregnated CaO sample was carbonated using CO_2. It seems that O_2 presence, during the CO oxidation-CO_2 capture processes, in the carbonation stage, allows a partial but continuous surface regeneration. On other words, the presence of O_2, as a reagent, should partially react with the metallic nickel, re-oxidizing it to NiO, and consequently eliminating the total catalytic deactivation. Thus, the catalytic performance was further preserved during the cycles and hydrogen production remained almost constant. Additionally, an unexpected hydrogen production was observed in cycles 2–5 between 500 and 550 °C, obtaining the highest H_2 formation (11.3%) during the cycle 5. The H_2 production, at a slightly lower temperature, may be produced by the two different nickel species produced during the CO oxidation step, Ni and NiO. Finally, the H_2 production performed at $T > 800$ °C corresponds to the CH_4 partial oxidation, as it was already described.

As it can be seen in Fig. 8(a), H_2 production remains constant in comparison with the cycles performed with the CO_2 chemisorption (Fig. 4). In this case, it is not necessary to perform an oxidative step, as the CO oxidation reaction must have induced a continuous

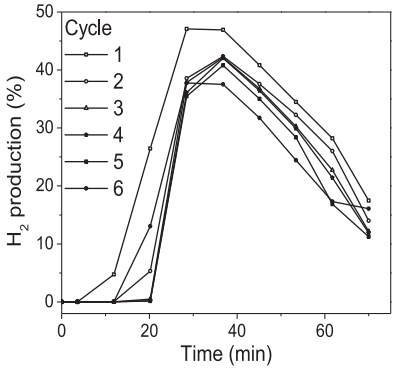

Fig. 9. Hydrogen evolution at 600 °C for six cycles of CO oxidation-CO_2 capture-dry reforming using the NiO-impregnated CaO sample.

nickel reoxidation. As expected, the X-ray pattern of the product obtained after six cycles was composed only by CaO and Ni metallic (Fig. 8(b)). These results show that it was possible to regenerate CaO ceramic after six consecutive cycles; however Ni species were reduced again to Ni metallic as consequence of H_2 production during the methane partial oxidation performed at high temperatures.

Once dynamic cyclic tests showed that it is possible to achieve the largest amounts of hydrogen around 600 °C using the NiO-impregnated CaO sample, isothermal cyclic experiments were undertaken at this value of temperature. Fig. 9 shows the hydrogen formation for six consecutive cycles. A similar catalytic behavior was observed in all isotherms, reaching the highest amount of H_2 after 37 min, followed by a decrease as a function of time, until productions between 11% and 17% were reached at 70 min of reaction time. In the first isotherm the highest amount of H_2 was obtained (47.1%, 29 min). After the first cycle, a decrease in the H_2 formation was observed for the following four cycles, until 40.7% of production was obtained in the fifth cycle at 37 min. Of course, the H_2 production depends on the CO_2 desorption from the ceramic. Thus, CH_4 reforming process is only produced while CaO is being decarbonated.

4. Conclusions

Two different CaO–NiO composites were tested as possible sequential CO_2 captors and catalytic materials for hydrogen production, thought consecutive CO_2 chemisorption and CH_4 reforming processes. The CH_4 reforming process, evaluated by the syngas production ($H_2 + CO$), was confirmed using both materials. Nevertheless, results clearly evidenced that NiO-impregnated CaO material always presented better chemical behaviors than CaO–NiO composite. Syngas was produced at different temperatures, between 400 and 600 °C and at $T > 800$ °C. In the first temperature range, the CH_4 reforming process was consistent with the CO_2 desorption. However the syngas produced at the highest temperature was not produced by the CH_4 reforming, but by the CH_4 partial oxidation. All these results were confirmed through different dynamic and isothermal cyclic experiments, as well as by the nickel reduction and carbon deposition evidenced by XRD.

A second set of experiments were performed using a CO–O_2 flow during the carbonation process, instead of CO_2. In this case, as it could be expected, a triple process was achieved: (i) CO oxidation, (ii) CO_2 chemisorption and (iii) CH_4 reforming. However, the hydrogen production was always higher than that obtained when CO_2 was used as carbon source. Hydrogen production enhancement was attributed to a partial but continuous catalyst surface regeneration produced by the oxygen presence. Based on these results, this kind of systems may be useful for designing specific systems, where CO or CO_2 is captured and used, as reagent, for the syngas production.

Acknowledgments

This work was financially supported by the projects PAPIIT-UNAM (IN-101916) and SENER-CONACyT. A. Cruz-Hernández thanks CONACyT and J. A. Mendoza-Nieto thanks DGAPA-UNAM for financial support. Authors thank A. Tejeda for technical help.

References

[1] P. Pall, T. Aina, D.A. Stone, P.A. Stott, T. Nozawa, A.G.J. Hilberts, D. Lohmann, M.R. Allen, Nature 470 (2011) 382–385.
[2] S.-K. Min, X. Zhang, F.W. Zwiers, G.C. Hegerl, Nature 470 (2011) 378–381.
[3] C.S. Martavaltzi, E.P. Pampaka, E.S. Korkakaki, A.A. Lemonidou, Energy Fuels 24 (2010) 2589–2595.
[4] D. Das, T.N. Veziroglu, Int. J. Hydrog. Energy 33 (2008) 6046–6057.
[5] A. Heinzel, B. Vogel, P. Hübner, J. Power Sour. 105 (2002) 202–207.
[6] T. Zhang, M.D. Amiridis, Appl. Catal. A 167 (1998) 161–172.
[7] J.R. Rostrup-Nielsen, T. Rostrup-Nielsen, Cattech 6 (2002) 150–159.
[8] S. Lin, M. Harada, Y. Suzuki, H. Hatano, Fuel 81 (2002) 2079–2085.
[9] S. Yaman, Energy Convers. Manag. 45 (2004) 651–671.
[10] S. Rapagna, Int. J. Hydrog. Energy. 23 (1998) 551–557.
[11] A.F. Lucrédio, E.M. Assaf, J. Power Sour. 159 (2006) 667–672.
[12] M.H. Halabi, J.M. De Croon, J. Van Der Schaaf, P.D. Cobden, J.C. Schouten, Chem. Eng. J. 168 (2011) 872–882.
[13] J.R. Hufton, S. Mayorga, S. Sircar, AIChE J. 45 (1999) 248–256.
[14] A. López Ortiz, M.A. Escobedo Bretado, J. Salinas Gutiérrez, M. Meléndez Zaragoza, R.H. Lara Castro, V. Collins Martínez, Int. J. Hydrog. Energy 40 (2015) 17192–17199.
[15] C. Zhao, Z. Zhou, Z. Cheng, X. Fang, Appl. Catal. B. 196 (2016) 16–26.
[16] K. Essaki, T. Muramatsu, M. Kato, Int. J. Hydrog. Energy 33 (2008) 6612–6618.
[17] R. Williams, Process Catalysis Synthesis, U.S. Pat. (1933) 1,909,442.
[18] W.B.R.E. Gorin, Method for the production of hydrogen, U.S. Pat. (1963) 3,108,857.
[19] J.A. Mendoza-Nieto, E. Vera, H. Pfeiffer, Chem. Lett. 45 (2016) 3–6.
[20] S. Wang, S. Yan, X. Ma, J. Gong, Energy Environ. Sci. 4 (2011) 3805.
[21] R.V. Siriwardane, C. Robinson, M. Shen, T. Simonyi, Energy Fuels 21 (2007) 2088–2097.
[22] E. Ochoa-Fernández, M. Rønning, T. Grande, D. Chen, Chem. Mater. 18 (2006) 1383–1385.
[23] H.A. Lara-García, M.J. Ramírez-Moreno, J. Ortiz-Landeros, H. Pfeiffer, RSC Adv. 6 (2016) 57880–57888.
[24] S.M. Amorim, M.D. Domenico, T.L.P. Dantas, H.J. José, R.F.P.M. Moreira, Chem. Eng. J. 283 (2016) 388–396.
[25] J.A. Mendoza-Nieto, H. Pfeiffer, RSC Adv. 6 (2016) 66579–66588.
[26] S.C. Lee, B.Y. Choi, C.K. Ryu, Y.S. Ahn, T.J. Lee, J.C. Kim, Korean J. Chem. Eng. 23 (2006) 374–379.
[27] G.S. Grasa, J.C. Abanades, Ind. Eng. Chem. Res. 45 (2006) 8846–8851.
[28] L. Li, X. Wen, X. Fu, F. Wang, N. Zhao, F. Xiao, W. Wei, Y. Sun, Energy Fuels 24 (2010) 5773–5780.
[29] A. Cruz-Hernández, B. Alcántar-Vázquez, J. Arenas, H. Pfeiffer, React. Kinet. Mech. Catal. 119 (2016) 445–455.
[30] S. Kumar, S.K. Saxena, Mater. Renew. Sustain. Energy 3 (2014) 30.
[31] J. Wang, L. Huang, R. Yang, Z. Zhang, J. Wu, Y. Gao, Q. Wang, D. O'Hare, Z. Zhong, Energy Environ. Sci. 7 (2014) 3478–3518.
[32] V. Manovic, E.J. Anthony, Environ. Sci. Technol. 43 (2009) 7117–7122.
[33] J.C. Abanades, E.J. Anthony, J. Wang, J.E. Oakey, Environ. Sci. Technol. 39 (2005) 2861–2866.
[34] Y.H. Hu, E. Ruckenstein, Catal. Lett. 36 (1996) 145–149.
[35] C. Han, D.P. Harrison, Chem. Eng. Sci. 49 (1994) 5875–5883.
[36] M. Specht, A. Bandi, F., Baumgart, T. Weimer, PCT Pat. WO01/23302 (2001).
[37] Y. Kato, K. Otsuka, C.Y. Liu, Chem. Eng. Res. Des. 83 (2005) 900–904.
[38] Y. Kato, K. Ando, Y. Yoshizawa, J. Chem. Eng. Jpn. 36 (2003) 860–866.
[39] L. Xu, H. Song, L. Chou, ACS Catal. 8 (2012) 1331–1342.
[40] V.R. Choudhary, A.M. Rajput, Ind. Eng. Chem. Res. 35 (1996) 3934–3939.
[41] V.R. Choudhary, A.M. Rajput, B. Prabhakar, Catal. Lett. 15 (1992) 363–370.
[42] Z.H. Lee, S. Ichikawa, K.T. Lee, A.R. Mohamed, J. Energy Chem. 24 (2015) 225–231.
[43] K. Johnsen, H.J. Ryu, J.R. Grace, C.J. Lim, Chem. Eng. Sci. 61 (2006) 1195–1202.
[44] S. Brun-Tsekhovoi, A.R. Zadorin, A.N. Katsobashvili, Y.R. Kourdyumov, in: Proceedings of the World Hydrogen Energy Conference, 1988, pp. 885–900.
[45] B. Balasubramanian, A. Lopez Ortiz, S. Kaytakoglu, D.P. Harrison, Chem. Eng. Sci. 54 (1999) 3543–3552.